Proteomic Analysis of Calcium- and Phosphorylation-dependent Calmodulin Complexes in Mammalian Cells

Deok-Jin Jang and Daojing Wang*

Life Sciences Division, Lawrence Berkeley National Laboratory, 1 Cyclotron Road, MS 84-171, Berkeley, CA 94720

*Correspondence to:

Dr. Daojing Wang
Life Sciences Division
Lawrence Berkeley National Laboratory
1 Cyclotron Road, MS 84-171
Berkeley, CA 94720

Tel: 510-486-6592
Fax: 510-486-4545
Email: djwang@lbl.gov

RUNNING TITLE: Proteomic analysis of calmodulin complexes

ABSTRACT

Protein conformational changes due to cofactor binding (e.g. metal ions, heme) and/or posttranslational modifications (e.g. phosphorylation) modulate dynamic protein complexes. Calmodulin (CaM) plays an essential role in regulating calcium (Ca^{2+}) signaling and homeostasis. No systematic approach on the identification of phosphorylation-dependent Ca^{2+}/CaM binding proteins has been published. Herein, we report a proteome-wide study of phosphorylation-dependent CaM binding proteins from mammalian cells. This method, termed "Dynamic Phosphoprotein Complex Trapping", "DPPC Trapping" for short, utilizes a combination of *in vivo* and *in vitro* assays. The basic strategy is to drastically shift the equilibrium towards endogenous phosphorylation of Ser, Thr, and Tyr at the global scale by inhibiting corresponding phosphatases *in vivo*. The phosphorylation-dependent calmodulin-binding proteins are then trapped *in vitro* in a Ca^{2+}-dependent manner by CaM-Sepharose chromatography. Finally, the isolated calmodulin-binding proteins are separated by SDS-PAGE and identified by LC/MS/MS. In parallel, the phosphorylation-dependent binding is visualized by silver staining and/or Western blotting. Using this method, we selectively identified over 120 CaM-associated proteins including many previously uncharacterized. We verified ubiquitin-protein ligase EDD1, inositol 1, 4, 5-triphosphate receptor type 1 (IP_3R1), and ATP-dependent RNA helicase DEAD box protein 3 (DDX3), as phosphorylation-dependent CaM binding proteins. To demonstrate the utilities of our method in understanding biological pathways, we showed that pSer/Thr of IP_3R1 *in vivo* by staurosporine-sensitive kinase(s), but not by PKA/PKG/PKC, significantly reduced the affinity of its Ca^{2+}-dependent CaM binding. However, pSer/Thr of IP_3R1 did not substantially affect its Ca^{2+}-indepedent CaM binding. We further showed that phosphatase PP1, but not PP2A or PP2B, plays a critical role in modulating the

phosphorylation-dependent CaM binding for IP_3R1. If combined with other phosphoprotein and phosphopeptide enrichment techniques such as IMAC, our method may serve as a general strategy to identify and characterize phosphorylation-dependent and functionally important protein complexes in mammalian cells.

KEYWORDS

Calmodulin, protein complexes, Ca^{2+}-dependent, phosphorylation-dependent, inositol 1, 4, 5-triphosphate receptor type 1 (IP_3R1), DEAD box protein 3 (DDX3), EDD1

INTRODUCTION

Metal ions and metalloproteins play important roles in regulating biological processes.[1] Calcium (Ca^{2+}) is the central second messenger. Ca^{2+} homeostasis and signaling is inherently linked to a myriad of cellular processes including cell growth, differentiation, synaptic activity, neurotransmitter release, and neuronal degeneration.[2] Calmodulin (CaM) is a ubiquitously expressed and highly conserved calcium regulatory protein. CaM binds up to four Ca^{2+} ions and interacts with its target proteins upon Ca^{2+} binding. Conformational changes occur in CaM upon its binding to Ca^{2+} and target proteins. Extensive research has been carried out to identify and characterize the Ca^{2+}/CaM complexes. For example, an online database (http://calcium.uhnres.utoronto.ca) exists for CaM targets. A recent proteome-wide scanning by using an mRNA-displayed human proteome library have identified around 100 proteins that potentially interact with CaM in a Ca^{2+}-dependent manner.[3]

Protein-protein interactions are vital for all cellular functions. Affinity purification-mass spectrometry remains one of the most powerful tools for the discovery and characterization of protein complexes.[4,5] Affinity approaches include classical immunoprecipitation, epitope-tagging with Flag or HA, GST-pull-down, and tandem affinity purification (TAP). Many protein interactions that are critical for cellular pathways are dynamic and tuned by posttranslational modifications. Thus, it is of the highest utility to have a means to "trap" dynamic complexes in order to identify and characterize them. Lowering the temperature has proven to be one of the most straightforward and generally applicable ways to trap protein complexes from hyperthermophilic Archaea like *P. furiosus* and *S. solfataricus*. However, more challenges remain for eukaryotic cells at ambient temperatures.

Protein phosphorylation and dephosphorylation at serine, threonine, and tyrosine are the predominant mechanisms of signal transduction in mammalian cells.[6-8] A global analysis of protein phosphorylation in yeast has been published.[9] Phosphorylation of CaM influences its binding to CaM-dependent proteins and results in important physiological consequences.[10] On the other hand, phosphorylation of its partners also affects the binding. For example, a recent study showed that phosphorylation of a protein named regulator of calmodulin signaling (RCS) at Ser55 by PKA increased its binding to CaM and led to inhibition of CaM-dependent phosphatase 2B (PP2B, also called calcineurin).[11] However, no systematic study on proteome-wide CaM-binding phosphoproteins has been published. The major hurdle lies in the low abundance of endogenous phosphorylated forms and the lack of an efficient way to trap these dynamic phosphorylation-dependent complexes.

We here describe a new strategy, termed "Dynamic Phosphoprotein Complex Trapping", "DPPC Trapping" for short, to identify and characterize calcium- and phosphorylation-dependent calmodulin complexes in mammalian cells. This method takes advantage of *in vivo* enrichment of endogenous phosphorylation of Ser, Thr, and Tyr, and *in vitro* trapping of the CaM complexes, followed by protein identification through LC/MS/MS. Our results demonstrate that "DPPC Trapping" is useful in identifying phosphorylation-dependent protein complexes and elucidating signaling pathways in mammalian cells.

EXPERIMENTAL PROCEDURES

Cell Culture

HeLa cells were grown in Dulbecco's modified Eagle's medium (DMEM) supplemented with 10% (v/v) fetal bovine serum (FBS) and penicillin/streptomycin in a humidified atmosphere of 5% (v/v) CO_2 at 37 °C. The cells were maintained overnight (16-18 hrs) in 1% FBS medium right before treatments. Cells with 70-80% confluency on 10 cm dishes were incubated with 100 μM sodium pervanadate (PV) for 2 hr and 20 nM calyculin A (CLA) for 1hr, respectively. To prepare stock solution of 50 mM sodium pervanadate, 100 mM sodium orthovanadate was activated by mixing 1:1 with 100 mM hydrogen peroxide. The reaction was allowed to proceed for 15 min at room temperature and terminated by addition of 400 U/ml of catalase. For kinase inhibitor experiments, cells were either treated with the desired inhibitor alone, or preincubated with the inhibitor followed by co-treatment with the inhibitor and 20 nM calyculin A for 1hr. The duration and concentration for each kinase inhibitor was: 30 min for 10 nM, 50 nM, 200 nM or 1 μM staurosporine, 1 hr for 2 μM chelerythrine, or 50 μM H-89, or 5 μM HA-1077, or 1 μM KT-5720, or 50 μM roscovitine. For protein phosphatase inhibitor experiments, the treatment was 1 hr for 10 μM cyclosporine A, or 200 nM okadaic acid, or 10 μM FK-506.

Protein kinase inhibitors including staurosporine (nonspecific for pSer/Thr kinases), H-89 (for PKA and PKG), chelerythrine (for PKC), HA-1077 (for Rho kinases), and roscovitine (for CDK1, 2, 5), were purchased from LC Labs, and KT-5720 (for PKA and phosphorylase) was from Calbiochem. Phosphatase inhibitors including calyculin A (for PP1 and PP2A), okadaic acid (for PP1 and PP2A), FK-506 (for PP2B), and cyclosporine A (for PP2B), were all purchased from LC Labs.

Sodium orthovanadate, hydrogen peroxide, and catalase were purchased from Sigma. Alkaline phosphatase was from New England Biolabs. Cell culture products and other consumable laboratory supplies were purchased from Fisher Scientific Corp. and VWR International. All other culture media and supplements were from Invitrogen.

Calmodulin Chromatography and Immunoblotting Analysis

HeLa cells were lysed with a lysis buffer containing 1% Triton X-100, 50 mM Tris–HCl (pH 7.5), 150 mM NaCl, 1 mM sodium pervanadate, 40 nM microcystin (Calbiochem), and protease inhibitor cocktails (Roche) in the presence of 2 mM $CaCl_2$ or 2 mM EGTA. To investigate the effects of *in vitro* auto-dephosphorylation on the CaM binding of IP_3R1, cells were lysed using buffers containing different combination of phosphatase inhibitors with other components remained unchanged. The conditions included pervanadate (PV) only, microcystin (MC) only, both of pervanadate and microcystin (PV+MC), in the absence of either inhibitor (-), and in the presence of alkaline phosphatase (AP, 50 unit/ml) only. The lysates were centrifuged at 15,000 rpm for 30 min at 4ºC by using a microcentrifuge. The protein concentration of the supernatants was quantified using the modified Bradford assay (Bio-Rad Laboratories). Resulted cell lysates were incubated at 4°C overnight with CaM Sepharose 4B beads (Amersham Biosciences) in the presence of 2 mM $CaCl_2$ or 2 mM EGTA. Subsequently, CaM beads were washed three times with the lysis buffer. Finally, proteins captured on beads were eluted and resolved by SDS–PAGE using 4-20% gels (ISC BioExpress), and subjected to silver staining or Western blot analysis.

For immunoblotting analysis, proteins separated on 4-20% gradient gels were transferred to a 0.45 μm nitrocellulose membrane (Bio-Rad Laboratories). The membrane was blocked with

5% nonfat milk, and incubated with the primary antibody in TBST buffer (25 mM Tris-HCl, pH 7.4, 60 mM NaCl, and 0.075% Tween 20) containing 5% nonfat milk. The bound primary antibodies were detected by a goat anti-mouse or a goat anti-rabbit IgG-horseradish peroxidase conjugate (Santa Cruz Biotechnologies) and the ECL detection system (Amersham Biosciences). The immunoblotting results were scanned with an Umax 2100 high-resolution scanner (Umax Technologies). The intensity of protein bands was quantified with ImageJ program (National Institutes of Health) and Student's t-test was used for statistical analysis.

The mouse monoclonal antibody against total actin (including all isoforms) was from Chemicon. The rabbit polyclonal anti-IP_3R1 antibody and the mouse monoclonal anti-phosphotyrosine (4G10) (p-Tyr) antibody were from Upstate. The rabbit polyclonal anti-phospho-threonine (p-Thr) antibody was from Cell Signaling. The goat anti-EDD1 antibody was from Santa Cruz Biotechnologies. The rabbit anti-DDX3 was from Bethyl Laboratories Inc.

In-Gel Digestion and Protein Identification

To identify CaM binding proteins, we followed essentially the same procedures as we described in detail previously for protein identification.[12] Briefly, a selected 22 silver-stained bands were excised from the gels and digested with trypsin. The tryptic peptides were extracted and subjected to LC/MS/MS analysis using a Q-TOF API US mass spectrometer (Waters Corp.) interfaced with a capillary liquid chromatography system (Waters Corp.). The LC eluent was directed to the electrospray source with a PicoTip emitter (New Objectives). Mass spectra were processed using MassLynx 4.0 software and proteins were identified using Protein Global Sever 1.0/2.0 software. The protein identities were further confirmed by Mascot (http://www.matrixscience.com) using the MS/MS peak lists exported from MassLynx. The

NCBI non-redundant databases were used for the search. For proteins with only one peptide sequenced, two criteria were used in the final identification following manual interpretation of the MS/MS data: Mascot score is more than 50, and the relative protein mobility on SDS-PAGE gels fits its theoretical molecular weight. Protein modifications considered included carbamidomethylation of cysteine (fixed), N-terminal acetylation, N-terminal Gln to pyroGlu, oxidation of methionine and phosphorylation of serine, threonine and tyrosine.

RESULTS

Calmodulin Binding was Ca^{2+}-dependent as well as Phosphorylation-dependent

Calyculin A (CLA) is a specific inhibitor for PP1 and PP2A, while pervanadate (PV) is a potent inhibitor for Tyr phosphatases. They have been used previously to increase *in vivo* global pSer/Thr and pTyr levels respectively.[13,14] Total lysates of HeLa cells treated with pervanadate for 2 hours or Calyculin A for 1 hour were compared to those of control cells. Western blotting using antibody that recognizes pThr or pTyr clearly showed drastic increase in global pSer/Thr and pTyr levels after CLA and PV treatments respectively (Figure 1A). To demonstrate that global protein expression was unaffected and to be assured of equal loading of total proteins, we stained the immunoblot with a ponceau solution (data not shown) and probed it with anti-actin antibody afterwards. Figure 1A clearly demonstrated the equal amount of actin indicating that global protein expression remained unchanged under our treatment conditions.

To identify phosphorylation-dependent CaM binding proteins, we carried out calmodulin chromatography in the presence of 2 mM $CaCl_2$ or 2 mM EGTA. The CaM binding products were separated by SDS-PAGE and detected by silver staining (Figure 1B). Twenty-two silver-stained bands labeled as 1 to 22 from the top to the bottom (Figure 1B) were selected for mass spectrometry analysis. These included Ca^{2+}-independent (Band 1 and Band 6) and Ca^{2+}-dependent bands (the remaining ones). There were multiple bands that showed clear phosphorylation-dependent binding to CaM, with band 3, 4 and 19 being downregulated and band 9 being upregulated after CLA treatment. Immunoblotting analysis of a duplicate gel using pTyr and pTyr antibodies respectively demonstrated that a significant number of these Ca^{2+}-dependent CaM-associated proteins are either pThr or pTyr proteins (data not shown).

Mass Spectrometry Identified Diverse Classes of Calmodulin Binding Proteins

All 22 silver-stained bands were identified successfully with high confidence using in-gel trypsin digestion followed by tandem mass spectrometry as described in Experimental Procedures. Majority of the bands contained more than one protein. For all the proteins identified, two search engines (ProteinLynx and Mascot) gave the same protein hits with high confident scores. A limited number of proteins were identified with only one peptide sequenced and manual interpretation of the MS/MS spectra (Mascot score > 50) was performed. In addition, the protein's predicted molecular weight agreed well with its relative mobility on the SDS-PAGE gel. The identity of the proteins, along with number of peptide sequenced and sequence coverage, and searched results using public databases for known CaM-binding motif and known phosphorylation, is listed in Table 1. For each band, proteins are listed in the order of descending Mascot scores. We have identified a significant number of CaM-associated proteins including those previously uncharacterized such as EDD1, DNA-PKcs, and several DEAD/H box proteins. A large portion of these proteins contain known CaM binding motifs and known pSer/Thr/Tyr sites (Table 1). Some of these proteins (e.g. CDC42) may have indirect-binding to CaM, i.e. piggypacking to CaM binding proteins (e.g. IQGAP1 for CDC42) and await future characterization. Proteins are further categorized as below.

Myosins. This is probably one of the best-characterized classes of CaM binding proteins. We identified myosin-9, myosin-6, myosin IE, and myosin IC. All of them contain IQ motif, which is a known Ca^{2+}-independent CaM binding motif. Interestingly, myosin IC is the major component of Band 9 which showed clear upregulation of CaM binding with an increase in Thr/Ser phosphorylation (i.e., CLA treatment).

Heat shock proteins. Most of the heat shock proteins we identified have known CaM-binding motif. These include heat shock 90 kDa protein 1 (1-5-10 motif), heat shock 70 kDa protein 9B (IQ motif), heat shock cognate 71 kDa protein (unclassified motif), and heat shock 70 kDa protein 1 (unclassified motif).

Kinases and phosphatases. Of particular interest is DNA-dependent protein kinase catalytic subunit (DNA-PKcs). It is the catalytic subunit of PI-3 kinase DNA-PK, which has two other components Ku70 and Ku80 and plays an essential role in the repair of DNA double-strand breaks (DSBs). To our knowledge, there was no previous report on CaM-binding of DNA-PKcs. Interestingly a potential IQ motif can be mapped to the DNA-PKcs sequence. This implicates that CaM and hence calcium signaling might be involved in DNA repair. Consistently, we also identified DNA damage binding protein 1, which is involved in the repair of UV-damaged DNA. Others kinases include CaM-kinase II, CaM-kinase 1D, 6-phosphofructokinase type C, 6-phosphofructo-2-kinase, and pyruvate kinase; while phosphatases include Ser/Thr protein phosphatase 5, Ser/Thr protein phosphatase 2A, and Ser/Thr protein phosphatase PP1.

DEAD/H-box proteins. These are generally ATP-dependent DNA or RNA helicase and are involved in a variety of cellular processes. We identified multiple Ca^{2+}/CaM-binding DEAD-box proteins including DDX11, DDX3, DDX49, and DDX47. Using mRNA-display, Shen et al. identified DDX5, DDX21, and DDX57 as Ca^{2+}/CaM-binding proteins.[3] Therefore, RNA unwinding through DDX proteins may be regulated by Ca^{2+}/CaM signaling.

Ribosomal proteins. These proteins interact with RNA in the ribosome and are involved in translation. We have identified 40S ribosomal proteins S3, S4, S8, and S5. Using mRNA-display, Shen et al. identified 40S ribosomal proteins S4, S8, S14, S15a, and 60S ribosomal

proteins L13a and L22.[3] These results suggest that Ca^{2+}/CaM may modulate ribosome assembly and translation through binding to ribosomal proteins.

14-3-3 proteins. These are a large family of approximately 30 kDa acidic proteins which exist primarily as homo- and heterodimeric within all eukaryotic cells. They mainly bind proteins containing phosphothreonine or phosphoserine motifs.[15] 14-3-3 proteins can directly regulate the catalytic activity of the bound protein, or regulate protein-protein interactions and subcellular localization of the bound protein. We have identified 14-3-3 protein zeta/delta, theta and gamma. However, further studies are needed to determine whether these proteins bind directly to CaM or are just piggypacking with Ca^{2+}/CaM-binding phosphoproteins.

Other proteins. These include elongation factors such as elongation factor 1 and elongation factor Tu; RNA binding proteins 14, FUS and polymerase delta-interacting protein 3; structural proteins such as gamma actin, alpha/beta tubulin and F-actin capping protein; metabolic enzymes such as ubiquitin-protein ligase, tRNA synthetase, phosphate synthetase, ATP synthase, ADP/ATP translocase, enolase, phosphodiesterase 1A, and phosphate dehydrogenase; heterogeneous nuclear ribonucleoproteins (hnRNP) such as hnRNP U, M, K, H, and A2/B1; and DNA replication licensing factor MCM7 (CDC47). Other proteins not described are tabulated in detail in Table 1.

To summarize, we have identified diverse classes of potentially Ca^{2+}-dependent CaM binding proteins that are involved in a myriad of signaling pathways. We also observed the phosphorylation-dependent CaM binding of several proteins including EDD1 (Band 3) and IP_3R1 (Band 4).

CLA Treatment Significantly Reduced Calmodulin Bindings of EDD1, IP_3R1, and DDX3

To further investigate the CaM binding patterns of EDD1 (Band 3), IP_3R1 (Band 4), and DDX3 (Band 13) discovered in the silver stain gel (Figure 1B), Western blotting was performed using antibodies specific to human EDD1, IP_3R1, DDX3, and actin respectively (Figure 2). Immunoblotting with anti-actin confirmed that equal amounts of total proteins were used in the CaM chromatography. Since actin does not binding directly to CaM, our results also indicated that the non-specific binding to Sepharose 4B beads during CaM chromatography was minimal. We showed that treatment with CLA or PV did not have any detectable effects on the expression levels of EDD1 and IP_3R1 (Input, Figure 2A). However, the Western band of DDX3 was slightly up-shifted and had consistently higher intensity after CLA treatment but not PV treatment (Input, Figure 2A). DDX3 is an ATP-dependent RNA helicase and localizes mostly in the nucleus. The up-shift is consistent with its mobility shift after phosphorylation by CLA treatment. It is known that DDX3 shuttles between the nucleus and the cytoplasm in a XPO1-dependent manner. Therefore, the apparent increase in the band intensity is probably due to the translocation of DDX3 from Triton-X insoluble to Triton-X soluble fraction after its phosphorylation. The binding of EDD1, IP_3R1, and DDX3 to calmodulin-sepharose in the presence of Ca^{2+} was dramatically reduced by CLA treatment when compared to the control (EDD1: 1.6 ± 1.9%, $P<0.001$, paired t-test, n=4; IP_3R1: 50.2 ± 14.4%, $P<0.001$, paired t-test, n=4; DDX3: 32.3 ± 8.8%, $P<0.001$, paired t-test, n=4), but not significantly affected by PV treatment (EDD1: 103.8 ± 8.0%, n=4; IP_3R1: 112.1 ± 6.6%, n=4; DDX3: 96.7 ± 10.5%, n=4) (Figure 2B). Since CLA significantly increased global pSer/Thr levels as shown in Figure 1A, this suggested that the reduction of *in vitro* CaM binding of IP_3R1, EDD1, and DDX3 are probably due to the elevation of their Ser/Thr phosphorylation *in vivo*. In presence of EGTA, the binding affinity between CaM and EDD1 and IP_3R1 was dramatically decreased. But in the case of DDX3, 50% of its

CaM binding affinity remained in the presence of EGTA. Similarly, CLA but not PV treatment significantly reduced this Ca^{2+}-independent CaM binding (CLA: 29.1 ± 4.5%; PV: 96.2 ± 22.6%).

Calmodulin Binding of IP_3R1 was pSer/Thr-dependent in the Presence of Ca^{2+}

To further confirm the pSer/Thr-dependent CaM binding of IP_3R1, we utilized a novel combination of *in vivo* and *in vitro* assays (Figure 3). This strategy takes advantage of the dephosphorylation by phosphatases *in vivo* (in cells) as well as *in vitro* (in cell lysates). It is well known that phosphatases remain active after cell lysis. We used CLA and microcystin to inhibit Ser/Thr phosphatases *in vivo* and *in vitro* respectively, while used pervanadate to inhibit Tyr phosphatases *in vitro*. Cells were lysed using buffers containing different combinations of phosphatase inhibitors as described in the Experimental Procedures. As confirmed in Figure 3B, CLA treatment significantly increased the global pSer/Thr levels (all lanes in Ctrl vs. corresponding ones in CLA), but this increase was substantially reduced during overnight incubation if microcystin was absent in the lysis buffer (- and PV lanes vs. MC and PV+MC lanes). In the presence of Ca^{2+}, the binding between CaM and IP_3R1 is reduced after *in vivo* CLA treatment in a pair-wise comparison using the same lysis buffer (Figure 3A and 3C). The binding reduction between IP_3R1 and CaM-sepharose was dramatically attenuated if microcystin was excluded from the lysis buffer. However, omission of pervanadate from the lysis buffer did not have substantial effects on the CaM binding of IP_3R1 (Figure 3A and 3C). This clearly suggested that pSer/Thr, but not pTyr, of IP_3R1 plays a major role in modulating its CaM binding. Further support for the dependence on pSer/Thr came from the alkaline phosphatase (AP lane) treatment experiments. Global dephosphorylation by alkaline phosphatase fully recovered the binding to

the basal level as in the control (Figure 3C). Interestingly, we also showed that the binding between IP_3R1 and CaM was not dependent on IP_3R1 phosphorylation in the absence of Ca^{2+} (EGTA lanes, Figure 3A and 3C), suggesting the complex interplay between Ca^{2+}-dependnet and phosphorylation-dependent binding between IP_3R1 and CaM.

Phosphorylation-dependent binding between IP_3R1 and calmodulin was regulated by staurosporine-sensitive kinase(s)

To further determine which kinase(s) modulate pSer/Thr-dependent CaM binding of IP_3R1, we have tested a series of kinase inhibitors (Figure 4). These inhibitors included: H-89, specific for PKA and less specific for PKG; chelerythrine (Che), specific for PKC; KT-5720 (KT), specific for PKA and phosphorylase kinase; HA-1077 (HA), specific for Rho kinases; roscovitine (RO), specific for CDK 1, 2, and 5; and staurosporine (ST), nonspecific for pSer/Thr kinases.

As shown in Figure 4, relative to the control, the CaM binding was significantly reduced in CLA alone (38.4 ± 7.5 %, n=7), reduced similarly with chelerythrine co-treatment (34.5 ± 1.5%, n=3), recovered half-way with H-89 co-treatment (61.9 ± 13.1%, n=3), and recovered fully with staurosporine co-treatment (116.9 ± 4.9%, n=3). No significant effect was observed for KT, HA, and RO treatments (35.7 ± 13.5%, 35.5 ± 13.6%, 34.9 ± 16.0%, n=3). At 50 μM, H-89 fully blocked PKA (IC_{50}= 48 nM), PKG (IC_{50}= 480 nM), and part of PKC (IC_{50}= 31.7 μM). However, the CLA-induced reduction in CaM binding was only partially blocked. Since inhibiting PKC with chelerythrine did not show any significant effects, other pSer/Thr kinase(s) in addition to PKA/PKG were probably involved. This was confirmed in the case of co-treatment with 1 μM staurosporine.

Interestingly, dose dependent recovery was observed only for staurosporine ranging from 10 nM to 1 μM (Figure 5). IC_{50} of staurosporine for PKA, PKC, and PKG is 7 nM, 0.7 nM, and 8.5 nM, respectively. Our data strongly suggested that other staurosporine-sensitive kinases, but not PKA/PKC/PKG, play a critical role in mediating the CLA-induced reduction of CaM binding of IP_3R1. We are actively pursuing the kinase(s) using RNA interference and overexpression of constitutively-active forms of potential kinase candidates.

Phosphorylation-dependent binding between IP_3R1 and CaM was regulated by phosphatase PP1

PP2B, in addition to PP1, was previously implicated in the dephosphorylation of neuronal IP_3R1 in neostriatal slices.[16] To further examine which phosphatase modulate pSer/Thr-dependent CaM binding of IP_3R1, we treated HeLa cells with 20 nM calyculin A (CLA), an inhibitor for PP1 and PP2A; or 200 nM okadaic acid (OA), an inhibitor for PP1 and PP2A; or 10 μM cyclosporine A (CsA), a PP2B inhibitor; or 10 μM FK506, another PP2B inhibitor. In contrast to CLA, CsA or FK506 treatment had no detectable effects on the CaM binding of IP_3R1 (CsA: 97.6% ± 4.0%, n=3; FK506: 107.3% ± 9.9%, n=3) (Figure 6). This suggested that either the basal PP2B in HeLa cells is not involved in the dephosphorylation of IP_3R1, or PP2B dephosphorylates pSer/Thr sites of IP_3R1 that are remote to the CaM-binding motif(s). We also showed that OA had much smaller effects than CLA (OA: 100.6% ± 10.9%, n=3). CLA and OA have a similar potency for PP2A, but OA is 100-fold less potent for PP1 than CLA. Therefore, our results strongly suggested that PP1 is the major phosphatase mediating phosphorylation-dependent CaM binding of IP_3R1.

DISCUSSION

It is increasingly clear that deciphering the complex mosaics of reversible protein assemblies in cellular pathways has become the central theme of systems biology. Cofactors such as metal ions regulate protein conformation and its functions. Given the critical role of protein phosphorylation and dephosphorylation in signal transduction of mammalian cells, it is essential to uncover the phosphorylation-dependent dynamic protein complexes in the context of biological pathways. In this study, we have showed that a new strategy "DPPC Trapping" is valuable in this endeavor. Using this strategy, we have successfully identified and verified multiple phosphorylation-dependent Ca^{2+}/CaM complexes in HeLa cells. Subsequent detailed studies of IP_3R1 have provided new insights into its *in vivo* regulation and biological functions.

"DPPC Trapping" takes advantage of the drastic increase of global endogenous pTyr and pSer/Thr levels after *in vivo* treatment with respective phosphatase inhibitors (Figure 7). Subsequent *in vitro* affinity purification such as immunoprecipitation with antibodies or CaM beads will pull down corresponding complexes resembling those *in vivo*. Finally the binding proteins and their phosphorylation sites will be identified by mass spectrometry and/or Western blotting. In parallel, the phosphorylation-dependent binding under different conditions can be quantified. To identify low-abundant phosphorylated proteins, a two-step sequential immunoprecipitation process may be carried out in the future. For example, the above IP products can be eluted with a buffer containing 2 mM EGTA, and the CaM-binding pTyr proteins can be further enriched using PT-66 (anti-pTyr) antibody. This extra step may help to determine whether the binding to CaM is Tyr-phosphorylation-dependent or -independent. The major concern of "DPPC Trapping" may be whether phosphorylation-dependent complexes resulted from phosphatase inhibitors treatment recapitulate the *in vivo* complexes under

physiological conditions. Nevertheless, "DPPC Trapping" serves as a discovery-driven strategy to identify potential candidates as dynamic phosphoprotein complexes. Further evidence will come from the identification of the phosphorylation site(s), the mapping of the binding domain(s), and the validation of protein-protein interaction using other techniques such as surface plasmon resonance (SPR)-a label free and sensitive method used to detect molecular interactions in real-time.[17] More insights into the phosphorylation-dependent binding will come from functional studies in the biological contexts.

Calmodulin plays a fundamental role in calcium homeostasis and signaling. Oxidation and phosphorylation of calmodulin has been shown to influence its binding to Ca^{2+}/CaM-dependent proteins and result in important physiological consequences.[10,18-20] However, no comprehensive studies on the phosphorylation status of Ca^{2+}/CaM binding partners have been published. We hypothesize that phosphorylation modulates calcium homeostasis and signaling through three types of phosphorylation-dependent Ca^{2+}/CaM complexes: phosphorylation-disabling (p-disabling), phosphorylation-enabling (p-enabling), and phosphorylation-modulating (p-modulating) (Figure 7). Using "DPPC Trapping", we have shown that binding of EDD1 and IP_3R1 to CaM is phosphorylation-disabling and that of myosin IC is phosphorylation-enabling. EDD1 is an E3 ubiquitin-protein ligase which accepts the ubiquitin from an E2 ubiquitin-conjugating enzyme in the form of a thioester and then directly transfers the ubiquitin to targeted substrates. It may be involved in the regulation of DNA topoisomerase II binding protein (TopBP1) for the DNA damage response.[21] To our knowledge, ours is the first report of the potential phosphorylation-dependent CaM binding of EDD1. As mentioned in the RESULTS section, we have also identified DNA-PKcs and DNA damage binding protein 1 as potential CaM-associated proteins. Taken together, Ca^{2+}/CaM may play an important role in DNA damage

response and repair, through association with DNA-PKcs, DNA damage binding protein 1, and EDD1, in a Ca^{2+}- and phosphorylation-dependent manner. Using mRNA display, Shen et al identified two CaM-binding deubiquitinating enzymes: ubiquitin C-terminal hydrolase UCHL5 and ubiquitin specific protease-M USP-M.[3] Therefore, Ca^{2+}/CaM may also regulate ubiquitin-proteasome pathways through differential bindings to ubiquitination-deubiquitination enzymes. We verified the pSer/Thr-dependent binding between DDX3 and CaM in a Ca^{2+}-dependent manner. Since DDX3 is an ATP-dependent RNA helicase, our results suggested potential roles of Ca^{2+} signaling in RNA unwinding.

IP_3 receptors (IP_3Rs) are critical Ca^{2+} release channels and respond to the second messenger IP_3. IP_3Rs are signal integrators that modulate a variety of cellular functions including contraction/excitation, secretion, gene expression, and cellular growth.[22] They are localized to a number of cellular membranes including endoplasmic reticulum (ER), Golgi apparatus, nucleoplasmic reticulum (NR), and plasma membrane (PM). IP_3R has three isoforms IP_3R 1-3 and IP_3R1 contains binding sites for IP_3, Ca^{2+}, CaM, Gβ, RACK1, myosin, CARP, 4.1N protein and cytochrome C.[22] IP_3R1 is phosphorylated by multiple kinases including: PKA and PKG at Ser1589 and 1756 in rats (corresponding to Ser1598 and Ser1764 in human, respectively);[23-25] PKC and CaM-kinase II at distinct sites;[26,27] AKT kinase at C-terminal tail S2681;[28] Cyclin-dependent kinase 1/cyclin B at Ser421 and Thr799;[29,30] and tyrosine kinases Fyn at Tyr 353,[31,32] and Lyn.[33] Protein phosphatase 1 and 2A form a macromolecular signaling complex with IP_3R1 and PKA and in turn regulate the phosphorylation and dephosphorylation of IP_3R1.[34] Extensive studies have demonstrated that calmodulin is a regulator of IP_3R and influences the binding of IP_3 to IP_3R.[35] For example, calmodulin was shown to bind to IP_3R1 in a Ca^{2+}-dependent manner and inhibit IP_3-induced calcium release.[36] More recently, a Ca^{2+}-dependent CaM binding motif

(aa1574-aa1595) was mapped to the functionally-important regulatory domain of IP_3R1;[37] while the other Ca^{2+}-independent CaM binding motif was mapped to its N-terminus.[38] Using an *in vitro* kinase reaction between PKA and lysates from COS cells transfected with short and long forms of rat IP_3R1, it was shown that CaM binding to the short form was reduced by 26% by *in vitro* PKA phosphorylation, while that to the long form was not significantly affected.[39] The selective impairment was attributed to the preferential phosphorylation of Ser1589 in the short form, which is adjacent to the CaM binding domain.[39,40] An earlier study has demonstrated that platelet IP_3R1 can be directly phosphorylated by endogenous membrane-associated kinases as well as exogenous PKA, and the phosphorylation differentially affected the IP_3-mediated Ca^{2+} release rate.[41] In this study, we showed that pSer/Thr (but not pTyr) of IP_3R1 significantly reduced its binding to Ca^{2+}/CaM. We demonstrated that staurosporine-sensitive kinase(s), but not PKA/PKG/PKC, played a critical role in modulating this binding. We further showed that phosphatase PP1, but not PP2A or PP2B, was involved in the binding reduction. IP_3R1 contains both Ca^{2+}-dependent (high affinity) and Ca^{2+}-independent (low affinity) CaM binding domains. Our method, we believe, for the first time showed that the former is phosphorylation-dependent while the latter is not. We are currently in the process of mapping the critical pSer/Thr site(s) and identifying the corresponding kinase(s). Taken together, our data suggested that phosphorylation of IP_3R1 inhibits its binding to CaM, promotes IP_3-induced Ca^{2+} release, and regulates Ca^{2+} signaling and homeostasis *in vivo.*

In conclusion, we have demonstrated the application of our "DPPC Trapping" method in identifying and characterizing Ca^{2+}- and phosphorylation-dependent dynamic protein complexes in mammalian cells. If combined with other phosphoprotein and phosphopeptide enrichment techniques such as phospho-specific IP and IMAC [42], this method may serve as a general

strategy to identify the protein complexes, map the phosphorylation sites, identify the corresponding kinases and phosphatases, and functionally characterize dynamic protein complexes *in vivo*.

ABBREVIATIONS: CaM, calmodulin; IP_3, inositol 1, 4, 5-trisphosphate; IP_3R1, IP_3 receptor 1; DEAD box protein 3, DDX3; PKA, protein kinase A, cAMP-dependent protein kinase; PKC, protein kinase C; PKG, protein kinase G, cGMP-dependent protein kinase; PP1, PP2A and PP2B, protein phosphatase 1, 2A and 2B; LC/MS/MS, liquid chromatography-tandem mass spectrometry; Q-TOF, quadrupole/time-of-flight

ACKNOWLEDEMENT

This work was supported by the Low Dose Radiation Research Program jointly funded by the U.S. Department of Energy and the National Aeronautics and Space Administration (NASA), and by grants GM077870 and HL079419 from the National Institutes of Health. This work was performed under the auspices of the U.S. Department of Energy, at the University of California/Lawrence Berkeley National Laboratory under contract no. DE AC02 05CH11231.

REFERENCES

(1) Finney, L. A.; O'Halloran, T. V. *Science* **2003**, *300*, 931-936.
(2) Berridge, M. J.; Bootman, M. D.; Roderick, H. L. *Nat Rev Mol Cell Biol* **2003**, *4*, 517-529.
(3) Shen, X.; Valencia, C. A.; Szostak, J. W.; Dong, B.; Liu, R. *Proc Natl Acad Sci U S A* **2005**, *102*, 5969-5974.
(4) Bauer, A.; Kuster, B. *Eur J Biochem* **2003**, *270*, 570-578.
(5) Gingras, A. C.; Aebersold, R.; Raught, B. *J Physiol* **2005**, *563*, 11-21.
(6) Hubbard, M. J.; Cohen, P. *Trends Biochem Sci* **1993**, *18*, 172-177.
(7) Hunter, T. *Cell* **2000**, *100*, 113-127.
(8) Cohen, P. *Trends Biochem Sci* **2000**, *25*, 596-601.
(9) Ptacek, J.; Devgan, G.; Michaud, G.; Zhu, H.; Zhu, X.; Fasolo, J.; Guo, H.; Jona, G.; Breitkreutz, A.; Sopko, R.; McCartney, R. R.; Schmidt, M. C.; Rachidi, N.; Lee, S. J.; Mah, A. S.; Meng, L.; Stark, M. J.; Stern, D. F.; De Virgilio, C.; Tyers, M.; Andrews, B.; Gerstein, M.; Schweitzer, B.; Predki, P. F.; Snyder, M. *Nature* **2005**, *438*, 679-684.
(10) Benaim, G.; Villalobo, A. *Eur J Biochem* **2002**, *269*, 3619-3631.
(11) Rakhilin, S. V.; Olson, P. A.; Nishi, A.; Starkova, N. N.; Fienberg, A. A.; Nairn, A. C.; Surmeier, D. J.; Greengard, P. *Science* **2004**, *306*, 698-701.
(12) Wang, D.; Park, J. S.; Chu, J. S.; Krakowski, A.; Luo, K.; Chen, D. J.; Li, S. *J Biol Chem* **2004**, *279*, 43725-43734.
(13) Shu, H.; Chen, S.; Bi, Q.; Mumby, M.; Brekken, D. L. *Mol Cell Proteomics* **2004**, *3*, 279-286.
(14) Rush, J.; Moritz, A.; Lee, K. A.; Guo, A.; Goss, V. L.; Spek, E. J.; Zhang, H.; Zha, X. M.; Polakiewicz, R. D.; Comb, M. J. *Nat Biotechnol* **2005**, *23*, 94-101.
(15) Yaffe, M. B. *FEBS Lett* **2002**, *513*, 53-57.
(16) Tang, T. S.; Tu, H.; Wang, Z.; Bezprozvanny, I. *J Neurosci* **2003**, *23*, 403-415.
(17) Lee, H. J.; Yan, Y.; Marriott, G.; Corn, R. M. *J Physiol* **2005**, *563*, 61-71.
(18) Bigelow, D. J.; Squier, T. C. *Biochim Biophys Acta* **2005**, *1703*, 121-134.
(19) Gao, J.; Yin, D.; Yao, Y.; Williams, T. D.; Squier, T. C. *Biochemistry* **1998**, *37*, 9536-9548.
(20) Greif, D. M.; Sacks, D. B.; Michel, T. *Proc Natl Acad Sci U S A* **2004**, *101*, 1165-1170.
(21) Honda, Y.; Tojo, M.; Matsuzaki, K.; Anan, T.; Matsumoto, M.; Ando, M.; Saya, H.; Nakao, M. *J Biol Chem* **2002**, *277*, 3599-3605.
(22) Patterson, R. L.; Boehning, D.; Snyder, S. H. *Annu Rev Biochem* **2004**, *73*, 437-465.
(23) Ferris, C. D.; Cameron, A. M.; Bredt, D. S.; Huganir, R. L.; Snyder, S. H. *Biochem Biophys Res Commun* **1991**, *175*, 192-198.
(24) Komalavilas, P.; Lincoln, T. M. *J Biol Chem* **1994**, *269*, 8701-8707.
(25) Wagner, L. E., 2nd; Li, W. H.; Yule, D. I. *J Biol Chem* **2003**, *278*, 45811-45817.
(26) Ferris, C. D.; Huganir, R. L.; Bredt, D. S.; Cameron, A. M.; Snyder, S. H. *Proc Natl Acad Sci U S A* **1991**, *88*, 2232-2235.
(27) Matter, N.; Ritz, M. F.; Freyermuth, S.; Rogue, P.; Malviya, A. N. *J Biol Chem* **1993**, *268*, 732-736.
(28) Khan, M. T.; Wagner, L., 2nd; Yule, D.; Bhanumathy, C.; Joseph, S. K. *J Biol Chem* **2005**, *[Epub ahead of print]*.

(29) Malathi, K.; Kohyama, S.; Ho, M.; Soghoian, D.; Li, X.; Silane, M.; Berenstein, A.; Jayaraman, T. *J Cell Biochem* **2003**, *90*, 1186-1196.
(30) Li, X.; Malathi, K.; Krizanova, O.; Ondrias, K.; Sperber, K.; Ablamunits, V.; Jayaraman, T. *J Immunol* **2005**, *175*, 6205-6210.
(31) Jayaraman, T.; Ondrias, K.; Ondriasova, E.; Marks, A. R. *Science* **1996**, *272*, 1492-1494.
(32) Cui, J.; Matkovich, S. J.; deSouza, N.; Li, S.; Rosemblit, N.; Marks, A. R. *J Biol Chem* **2004**, *279*, 16311-16316.
(33) Yokoyama, K.; Su Ih, I. H.; Tezuka, T.; Yasuda, T.; Mikoshiba, K.; Tarakhovsky, A.; Yamamoto, T. *Embo J* **2002**, *21*, 83-92.
(34) DeSouza, N.; Reiken, S.; Ondrias, K.; Yang, Y. M.; Matkovich, S.; Marks, A. R. *J Biol Chem* **2002**, *277*, 39397-39400.
(35) Patel, S.; Joseph, S. K.; Thomas, A. P. *Cell Calcium* **1999**, *25*, 247-264.
(36) Hirota, J.; Michikawa, T.; Natsume, T.; Furuichi, T.; Mikoshiba, K. *FEBS Lett* **1999**, *456*, 322-326.
(37) Yamada, M.; Miyawaki, A.; Saito, K.; Nakajima, T.; Yamamoto-Hino, M.; Ryo, Y.; Furuichi, T.; Mikoshiba, K. *Biochem J* **1995**, *308 (Pt 1)*, 83-88.
(38) Sienaert, I.; Nadif Kasri, N.; Vanlingen, S.; Parys, J. B.; Callewaert, G.; Missiaen, L.; de Smedt, H. *Biochem J* **2002**, *365*, 269-277.
(39) Lin, C.; Widjaja, J.; Joseph, S. K. *J Biol Chem* **2000**, *275*, 2305-2311.
(40) Danoff, S. K.; Ferris, C. D.; Donath, C.; Fischer, G. A.; Munemitsu, S.; Ullrich, A.; Snyder, S. H.; Ross, C. A. *Proc Natl Acad Sci U S A* **1991**, *88*, 2951-2955.
(41) Quinton, T. M.; Brown, K. D.; Dean, W. L. *Biochemistry* **1996**, *35*, 6865-6871.
(42) Ficarro, S. B.; McCleland, M. L.; Stukenberg, P. T.; Burke, D. J.; Ross, M. M.; Shabanowitz, J.; Hunt, D. F.; White, F. M. *Nat Biotechnol* **2002**, *20*, 301-305.

FIGURE CAPTIONS

Figure 1. Western blot analysis of HeLa cells after phosphatase inhibitors treatments (A) and silver staining of proteins bound to calmodulin-sepharose (B). (A) Cell lysates were separated on 4-20% SDS-PAGE gels and blotted to nitrocellulose membranes. Total protein loaded per lane was 30 μg for cells either untreated (Ctrl), or treated with 20 nM calyculin A (CLA) for 1 hr, or 100 μM pervanadate (PV) for 2 hr. The blots were probed with anti-pThr (left), anti-pTyr (center), and anti-actin (right), respectively. (B) The CaM chromatography was carried out in the presence of Ca^{2+} or EGTA, and the binding products from a total of 2 x 10^6 HeLa cells were compared in each lane. Gels were stained with silver nitrate. Twenty-two bands as labeled were cut out for mass spec analysis.

Figure 2. The binding of EDD1, IP_3R1, and DDX3 to calmodulin-sepharose. (A) A representative Western blot. (B) Quantitation of band intensity in the Western blots. The values were normalized to corresponding untreated controls and expressed as Mean ± S.D. (n=4). Error bar indicates the standard deviation (S.D.). HeLa cells were either untreated (Ctrl), or treated with 20 nM calyculin A (CLA) for 1 hr, or 100 μM pervanadate (PV) for 2 hr. 30 μg of total cell lysates were directly analyzed as input. The CaM chromatography was carried out in the presence of Ca^{2+} or EGTA, and the binding products from a total of 2 x 10^6 HeLa cells were compared in each lane. The blots were probed with anti-EDD1, anti-IP_3R1, anti-DDX3, and anti-actin (as negative control) antibody, respectively.

Figure 3. pSer/Thr-dependent binding of IP_3R1 to calmodulin-sepharose in a Ca^{2+}-dependent manner. Representative Western blots of CaM binding products (A) and of corresponding total

cell lysates (B). (C) Quantitation of band intensity in the Western blots (A). The values were normalized to corresponding untreated controls with no inhibitors in the lysis buffer and expressed as Mean ± S.D. (n=4). Error bar indicates the standard deviation (S.D.). HeLa cells were either untreated (Ctrl) or treated with 20 nM calyculin A (CLA) for 1 hr, and then lysed using lysis buffers containing pervanadate (PV) only, or microcystin (MC) only, or both (PV+MC), or in the absence of inhibitors (-), or in the presence of alkaline phosphatase (AP, 50 unit/ml) only. The CaM chromatography was carried out in the presence of Ca^{2+} or EGTA. The blots were probed with anti-IP_3R1 (A) and p-Thr (B) antibody respectively.

Figure 4. The effects of protein kinase inhibitors on the binding of IP_3R1 to calmodulin-sepharose. (A) A representative Western blot of CaM binding products. (B) Quantitation of the band intensity in the Western blots. The values were normalized to the untreated control and expressed as Mean ± SD. Error bar indicates standard deviation (S.D.). HeLa cells were either untreated, or treated with CLA alone, or treated with an inhibitor followed by the co-treatment with CLA. The data were analyzed for the control (Ctrl, n=7); 20 nM calycuin A alone (CLA, n=7); and inhibitor co-treatment with CLA plus 1 μM staurosporine (ST+CLA, n=3); 50 μM H-89 (H-89+CLA, n=3); 2 μM chelerythrine (Che+CLA, n=3); 1 μM KT-5720 (KT+CLA, n=3); 5 μM HA-1077 (HA+CLA, n=3); and 50 μM roscovitine (RO+CLA, n=3). The blot was probed with an anti-IP_3R1 antibody.

Figure 5. The effects of staurosporine (ST) on the binding of IP_3R1 to calmodulin-sepharose in a dose-dependent manner. (A) A representative Western blot of CaM binding products. (B) Quantitation of the band intensity in the Western blots. The values were normalized to the

untreated control and expressed as Mean ± SD. Error bar indicates standard deviation (S.D.). HeLa cells were either untreated or treated with 20 nM calyculin A (CLA) alone, or co-treated with different concentrations of ST (10-1000 nM) as specified. The blot was probed with an anti-IP_3R1 antibody.

Figure 6. The effects of protein phosphatase inhibitors on the binding of IP_3R1 to calmodulin-sepharose. (A) A representative Western blot of CaM binding products. (B) Quantitation of IP_3R1 band intensities in the Western blots. The values were normalized to the untreated control and expressed as Mean ± SD (n=3). Error bar indicates standard deviation (S.D.). HeLa cells were either untreated (Ctrl), or treated with 20 nM calyculin A (CLA), or 200 nM okadaic acid (OA), 10 μM FK-506, or 10 μM cyclosporine A (CsA) for 1 hr. The blot was probed with an anti-IP_3R1 antibody.

Figure 7. A scheme showing the "DPPC Trapping" method and three kinds of phosphorylation-dependent dynamic CaM complexes. The basic strategy is to drastically shift the equilibrium towards endogenous phosphorylation of Ser, Thr, and Tyr at the global scale by inhibiting corresponding phosphatases *in vivo*. The phosphorylation-dependent including phosphorylation-disabling (p-disabling), phosphorylation-enabling (p-enabling), and phosphorylation-modulating (p-modulating) complexes are then trapped *in vitro* in a Ca^{2+}-dependent manner by calmodulin immunoprecipitation. Finally, the isolated calmodulin-binding proteins are separated by SDS-PAGE and identified by LC/MS/MS. In parallel, the phosphorylation-dependent binding is visualized by silver staining and/or Western blotting. Protein complex candidates can be further verified and characterized through a combination of *in vivo* and *in vitro* assays.

Table 1: Potential Ca^{2+}/CaM Binding Proteins isolated from HeLa cells

Band No.	Protein name	No. of peptide sequenced	Sequence coverage	Swiss- Prot accession No.	Molecular mass (kDa)	Known CaM-binding motif [a]	Known Phosphorylation [c]
	Retinoblastoma-associated factor 600	29	7%	Q5T4S7	573.8	-	-
1	Plectin 1	7	2%	Q15149	531.7	IQ	+
2	DNA-dependent protein kinase catalytic subunit (DNA-PKcs)	3	1%	P78527	469.1	IQ	+
3	Ubiquitin-protein ligase EDD1	18	10%	O95071	309.4	IQ	+
	Inositol 1,4,5-trisphosphate receptor type 1	40	21%	Q14643	313.9[d]	1-14, 2 Unclassified	+
	Filamin-A	20	12%	P21333	280.7	-	+
	Spectrin alpha chain	11	7%	Q13813	284.5	-	+
4	Inositol 1,4,5-trisphosphate receptor type 3	10	6%	Q14573	304.0	2 IQ	+[b]
	Spectrin beta chain	2	1%	Q01082	274.6	IQ	+
	CREB-binding protein (CBP)	2	1%	Q92793	265.3	IQ	+
	Centrosome protein Cep290	2	1%	Q66GS8	290.3	-	-
	Myosin-9	46	29%	P35579	226.4	IQ[b]	+
5	Girdin	4	3%	Q3V6T2	215.9	Unclassified	-
	Ras GTPase-activating like protein IQGAP1	76	55%	P46940	189.2	4 IQ[b]	+
	TBC1 domain family member 4	7	7%	O60343	146.6	-	+
6	Bifunctional aminoacyl-tRNA synthetase	3	2%	P07814	163.1	IQ	+
	Kinesin-like protein 2	2	1%	Q9NS87	160.2	Unclassified	-
	Leucine-rich PPR-motif containing protein	14	13%	P42704	145.2	-	-
	Neuropathy target esterase	12	13%	O60859	146.2	-	-
	Myosin-6	8	8%	Q9UM54	148.7	IQ[b]	+
7	Carbamoyl-phosphate synthetase I	6	4%	P31327	164.9	-	-
	Kinesin-like protein KIF1C	7	7%	O43896	123.1	-	-
	Formin-like 1 protein	2	3%	O95466	121.8	-	-
	Golgin subfamily A member 2	1	1%	Q08379	111.7	-	+
	Myosin IE	21	18%	Q12965	127.0	IQ	-
8	DNA damage binding protein 1	3	4%	Q16531	126.9	-	-
	Myosin IC	31	34%	O00159	118.0	3 IQ[b]	+
9	Heterogeneous nuclear ribonucleoprotein U	3	6%	Q00839	90.4	-	+
	DDX11 protein	3	4%	Q86W62	108.3	-	-
10	Heat shock 90 kDa protein 1, beta	2	3%	Q5T9W7	83.3	1-5-10	-
	DNA replication licensing factor MCM7	15	22%	P33993	81.3	-	-
11	6-phosphofructokinase type C	6	9%	Q01813	85.6	-	+

	RED protein	11	27%	Q13123	65.6	-	-
	Trifunctional enzyme alpha subunit	10	20%	P40939	83.0	-	-
	78 kDa glucose-regulated protein	7	17%	P11021	72.3	IQ	-
	Glycerol-3-phosphate dehydrogenase	9	18%	P43304	80.8	-	-
12	Long-chain-fatty-acid--CoA ligase 4	6	11%	O60488	79.2	-	-
	Heterogeneous nuclear ribonucleoprotein M	4	7%	P52272	77.4	-	+
	Lamin A/C	3	6%	P02545	74.1	-	+
	Heat shock 70 kDa protein 9B	5	8%	Q6GU03	73.7	IQ	-
	Heat shock cognate 71 kDa protein	17	34%	P11142	70.9	Unclassified	+
	Heat shock 70 kDa protein 1	9	23%	P08107	70.0	Unclassified	+
	RNA binding protein 14	8	15%	Q96PK6	69.5	-	+[b]
13	DEAD-box protein 3	6	12%	O00571	73.1	-	+
	Melanoma-associated antigen D2	6	16%	Q9UNF1	64.9	Unclassified	+
	Calcium-binding mitochondrial carrier protein Aralar2	6	16%	Q9UJS0	74.2	-	-
	Calcium/calmodulin-dependent 3',5'-cyclic nucleotide phosphodiesterase 1A	8	20%	P54750	61.1	1-12	-
	RNA-binding protein Fus	9	16%	P35637	53.4	-	+
	Pyruvate kinase, isozymes M1/M2	6	16%	P14618	57.8	-	-
	CaM-kinase II gamma chain	3	8%	Q13555	62.6	-	+
	Non-POU domain-containing octamer-binding protein	5	15%	Q15233	54.2	-	-
	Heterogeneous nuclear ribonucleoprotein K	3	10%	P61978	51.0	-	+[b]
14	Nucleolar complex protein 4 homolog	3	9%	Q9BVI4	58.5	-	-
	PAP associated domain containing 1	2	5%	Q6P7E5	66.2	-	-
	Phenylalanyl-tRNA synthetase alpha chain	1	2%	Q9Y285	57.4	Unclassified	-
	COP9 signalosome complex subunit 1	2	4%	Q13098	53.4	-	-
	D-3-phosphoglycerate dehydrogenase	3	6%	O43175	56.5	IQ	-
	Serine/threonine protein phosphatase 5	1	4%	P53041	56.9	-	-
	SH2D4A protein	2	5%	Q5XKC1	52.7	-	-
	ATP synthase alpha chain	6	15%	P25705	59.8	Unclassified	+
	ATP synthase beta chain	3	8%	P06576	56.6	-	-
	Probable ATP-dependent RNA helicase	5	15%	Q9Y6V7	54.2	-	-
15	DDX49						
	Seryl-tRNA synthetase	2	6%	Q9NP81	58.3	IQ	-
	Plasminogen activator inhibitor 1 RNA-binding protein	1	4%	Q8NC51	44.9	IQ	+
	Tubulin beta	16	40%	P07437	49.7	-	+
	Tubulin alpha-6 chain	10	33%	Q9BQE3	49.9	-	-
	Tubulin beta-6 chain	8	20%	Q9BUF5	49.9	-	-
	NOL1/NOL2/SUN domain family, member 5,	10	24%	Q96HT9	50.4	-	+
16	isoform 1						-
	Chromatin assembly factor 1 subunit C	2	6%	Q09028	47.5	-	-
	RuvB-like 2	2	5%	Q9Y230	51.0	-	+
	CaM-kinase II delta chain	1	2%	Q13557	56.3	1-5-10	+
	Heterogeneous nuclear ribonucleoprotein H	1	3%	P31943	49.1	-	-
	Serine/threonine protein phosphatase 2A, 55 kDa regulatory subunit B, alpha isoform	2	5%	P63151	51.7	-	-
	SWI/SNF-related matrix-associated actin-	1	3%	Q969G3	46.6	IQ	-

	dependent regulator of chromatin E1						
	Probable ATP-dependent RNA helicase DDX47	1	3%	Q9H0S4	50.6	-	-
	Alpha-enolase	3	9%	P06733	47.0	-	+
	6-phosphofructo-2-kinase	1	2%	Q5VVQ3	54.4	-	-
	Elongation factor 1-alpha 1	8	20%	P68104	50.1	-	+
	Polymerase delta-interacting protein 3	4	15%	Q9BY77	46.1	-	+
	Trifunctional enzyme beta subunit	3	6%	P55084	51.4	IQ	-
	Elongation factor Tu	2	5%	P49411	49.5	-	-
	Protein TFG	3	9%	Q92734	43.4	-	-
17	Methionine adenosyltransferase II, alpha	1	3%	Q53SP5	43.7	-	-
	Splicing factor 3B subunit 4	1	3%	Q15427	44.4	-	+
	Elongation factor 1-gamma	1	2%	P26641	49.9	Unclassified	-
	Eukaryotic translation initiation factor 4A, isoform 2	1	3%	Q53XJ6	46.4	Unclassified	-
	Gamma-actin	14	47%	P63261	41.8	-	-
	Stomatin-like protein 2	6	30%	Q9UJZ1	38.5	-	+
	RNA (guanine-9-) methyltransferase domain	5	15%	Q9NRG5	47.3	-	-
18	containing 1 (HNYA)						
	Calcium/calmodulin-dependent protein kinase type 1D	2	8%	Q8IU85	42.9	1-14	+
	Annexin A2	11	33%	P07355	38.5	Unclassified	+
	Protein kinase C, delta binding protein	7	45%	Q969G5	27.6	IQ	-
	Glyceraldehyde-3-phosphate dehydrogenase	5	17%	P04406	35.9	-	+
	BLOCK 23	4	14%	Q8NHW5	34.4	-	-
	F-actin capping protein alpha-1 subunit	3	14%	P52907	32.9	-	-
19	Heterogeneous nuclear ribonucleoproteins A2/B1	2	7%	P22626	37.4	-	+
	Ser/Thr protein phosphatase PP1-alpha	1	5%	P62136	37.5	-	+
	Protein C20orf77	1	4%	Q9NQG5	36.9	-	+
	L-lactate dehydrogenase A chain	1	4%	P00338	36.6	-	+
	ATP synthase gamma chain	5	25%	P36542	33.0	-	-
20	Prostaglandin E synthase 2 (Truncated)	2	15%	Q9H7Z7	29.2	-	-
	40S ribosomal protein S3	3	16%	P23396	26.7	-	+
	40S ribosomal protein S4, X isoform	6	18%	P62701	29.5	-	-
	ADP/ATP translocase 2	6	18%	P05141	32.8	-	-
	14-3-3 protein zeta/delta	4	22%	P63104	27.8	-	+
	Pyrroline-5-carboxylate reductase-like	3	13%	Q96HX4	28.6	-	-
	UPF0082 protein PRO0477	4	28%	Q9BSH4	32.5	-	-
	Protein C21orf70	2	11%	Q9NSI2	25.5	-	-
21	14-3-3 protein theta	2	13%	P27348	27.8	-	+
	Ribosomal protein S8	1	6%	Q5JR95	21.9	-	-
	14-3-3 protein gamma	1	5%	P61981	28.2	-	-
	Osteoclast stimulating factor 1 variant	1	5%	Q5W126	23.8	-	-
	Cytochrome C-1	1	4%	Q5U062	35.4	-	-
	Proteasome subunit alpha type 7	1	5%	O14818	27.9	-	-
	SCO1 protein homolog	1	8%	O75880	33.8	-	-
	Cell division control protein 42 homolog	4	24%	P60953	21.3	-	+

22	(CDC42)						
	40S Ribosomal protein S5	3	22%	P46782	22.7	-	-
	Rho family GTPase Chp	1	4%	Q96L33	26.2	-	-

[a] Note: Searched through: http://calcium.uhnres.utoronto.ca
[b] Note: Searched through: http://us.expasy.org/sprot/
[c] Note: Searched through: http://www.phosphosite.org
[d] Note: Theoretical molecular weight for the full length IP_3R1 (i.e. long form)

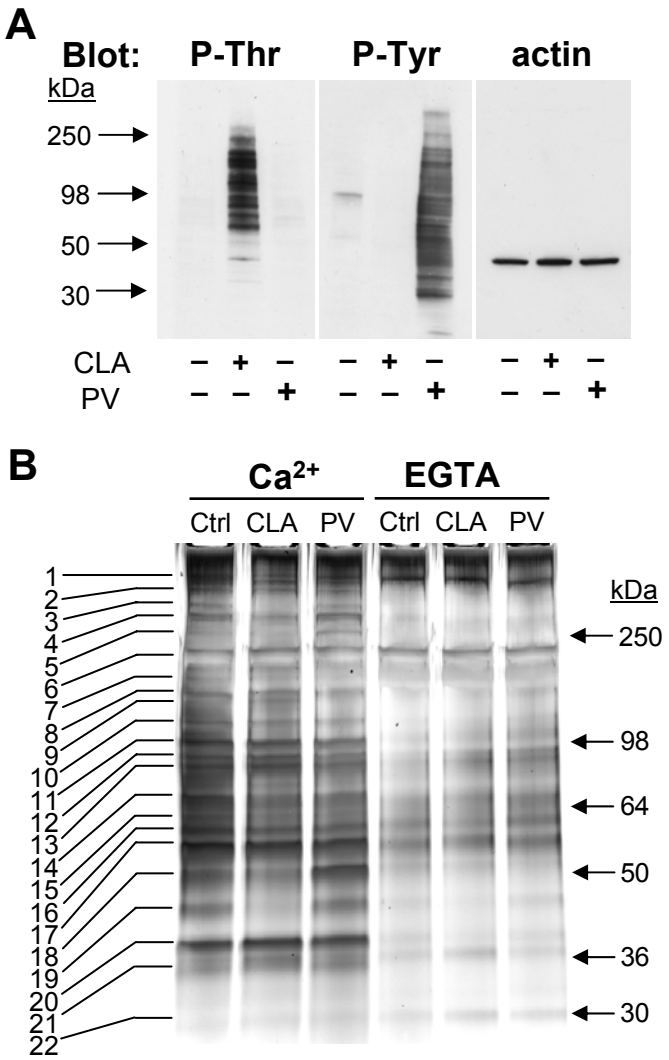
A
Blot:
P-Thr
P-Tyr
actin
kDa
250
98
50
30
CLA
PV
B
Ca2+
EGTA
Ctrl
CLA
PV
Ctrl
CLA
PV
kDa
250
98
64
50
36
30
1
2
3
4
5
6
7
8
9
10
11
12
13
14
15
16
17
18
19
20
21
22

Figure 1

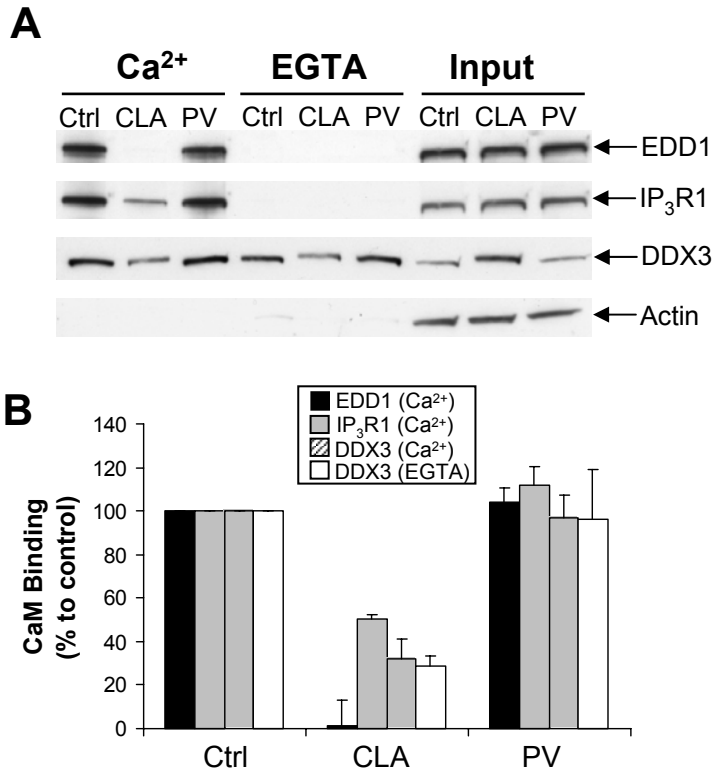
A
Ca2+
EGTA
Input
Ctrl CLA PV Ctrl CLA PV Ctrl CLA PV
EDD1
IP3R1
DDX3
Actin
B
EDD1 (Ca2+)
IP3R1 (Ca2+)
DDX3 (Ca2+)
DDX3 (EGTA)
CaM Binding (% to control)
140
120
100
80
60
40
20
0
Ctrl
CLA
PV

Figure 2

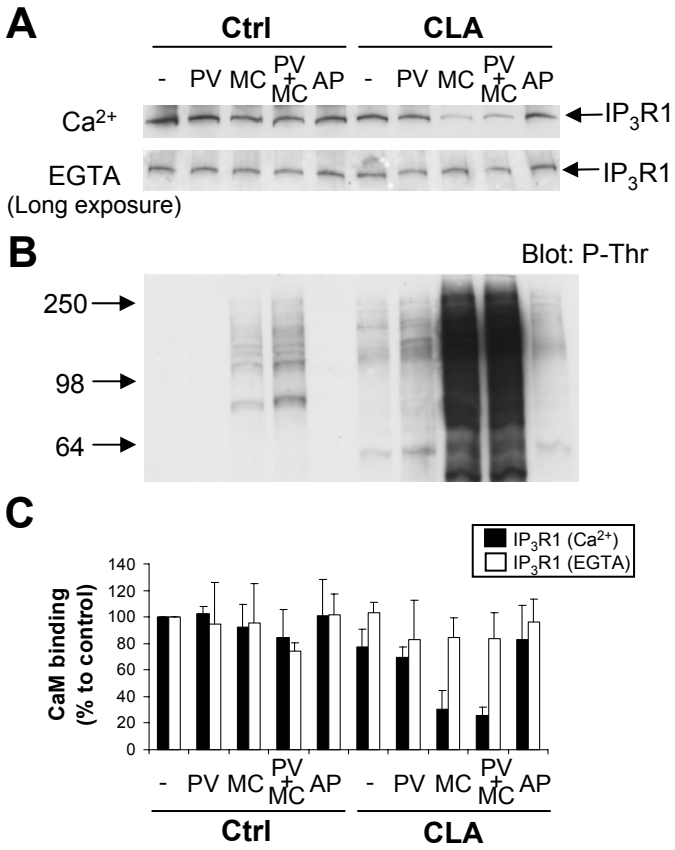
A
Ctrl
CLA
- PV MC PV + MC AP - PV MC PV + MC AP
Ca2+
IP3R1
EGTA
IP3R1
(Long exposure)
B
Blot: P-Thr
250
98
64
C
IP3R1 (Ca2+)
IP3R1 (EGTA)
CaM binding (% to control)
140
120
100
80
60
40
20
0
- PV MC PV + MC AP - PV MC PV + MC AP
Ctrl
CLA

Figure 3

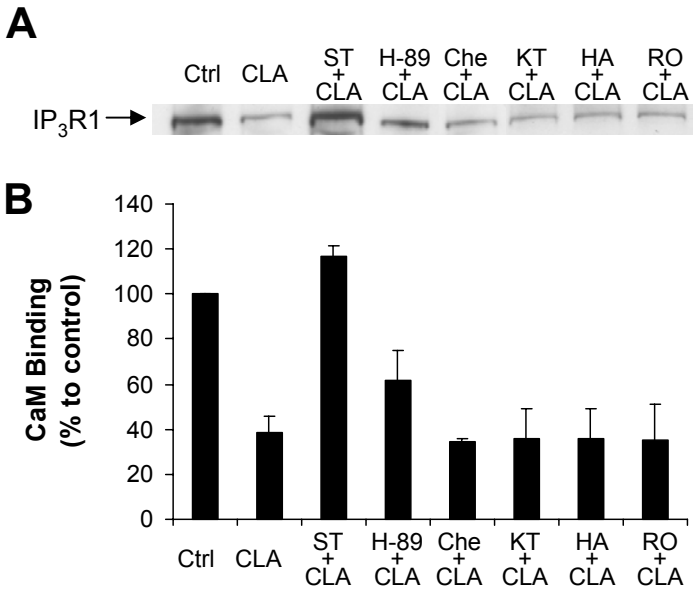
A
Ctrl
CLA
ST + CLA
H-89 + CLA
Che + CLA
KT + CLA
HA + CLA
RO + CLA
IP3R1
B
CaM Binding (% to control)
140
120
100
80
60
40
20
0
Ctrl
CLA
ST + CLA
H-89 + CLA
Che + CLA
KT + CLA
HA + CLA
RO + CLA

Figure 4

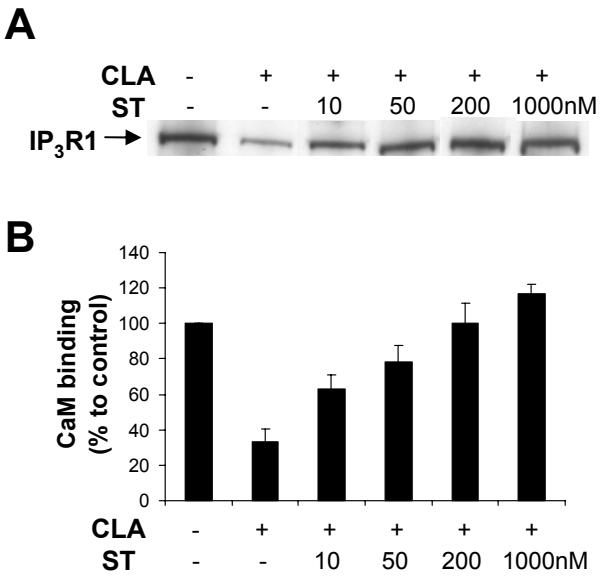
A
CLA - + + + + +
ST - - 10 50 200 1000nM
IP3R1
B
CaM binding (% to control)
140
120
100
80
60
40
20
0
CLA - + + + + +
ST - - 10 50 200 1000nM

Figure 5

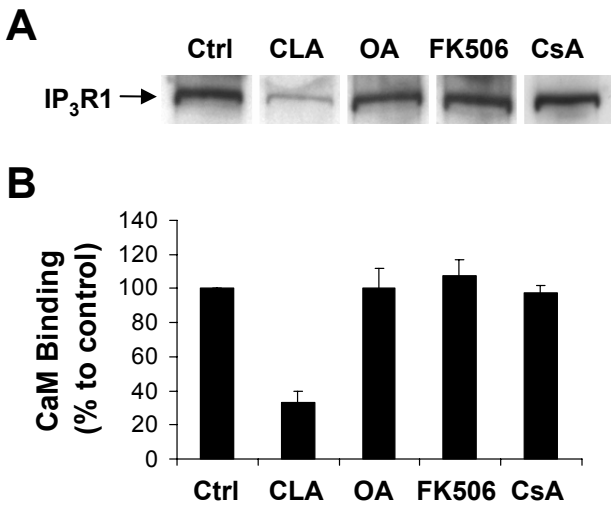
A
Ctrl
CLA
OA
FK506
CsA
IP3R1
B
CaM Binding
(% to control)
140
120
100
80
60
40
20
0
Ctrl
CLA
OA
FK506
CsA

Figure 6

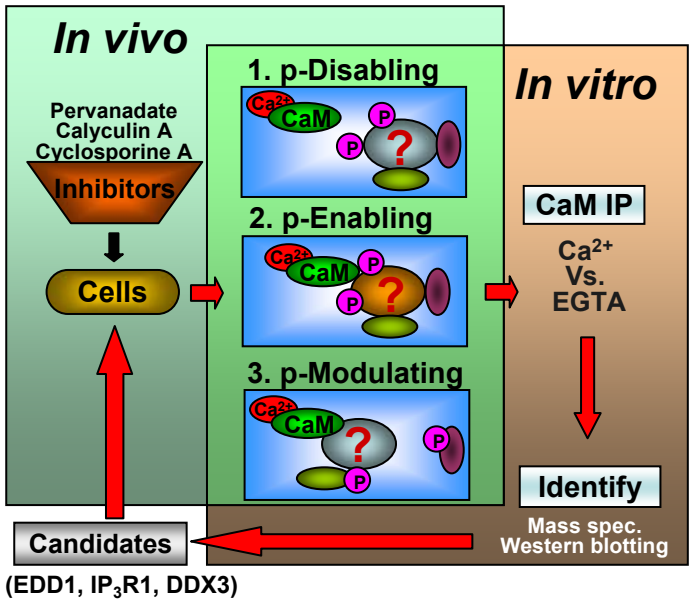
In vivo
Pervanadate
Calyculin A
Cyclosporine A
Inhibitors
Cells
1. p-Disabling
2. p-Enabling
3. p-Modulating
Ca2+
CaM
P
?
In vitro
CaM IP
Ca2+
Vs.
EGTA
Identify
Mass spec.
Western blotting
Candidates
(EDD1, IP3R1, DDX3)

Figure 7